American Mineralogist, Volume 78, pages 377–390, 1993

The characterization of mafic phyllosilicates in low-grade metabasalts from eastern North Greenland

D. Robinson
Department of Geology, Wills Memorial Building, University of Bristol, Queen's Road, Bristol BS8 1RJ, England
R. E. Bevins
Department of Geology, National Museum of Wales, Cardiff CF1 3NP, Wales
G. Rowbotham
Department of Geology, University of Keele, Keele, Staffordshire ST5 5BG, England

Abstract

Utilizing a combination of petrographic, XRD, and microprobe data, a progressive sequence of mafic phyllosilicates from random mixed-layer chlorite/smectite (ca. 25% chlorite) through different types of regular mixed-layer chlorite/smectite (ca. 60, 65, 80, and 85% chlorite) to discrete chlorite has been identified in basalts affected by low-grade regional metamorphism from the late Proterozoic Zig-Zag Dal Basalt Formation of eastern North Greenland. Considerable variation in composition is present in these mafic phyllosilicates, which is shown to be attributable in part to very fine-grained physical intergrowths between coexisting phases and also to a tendency toward a di-, trioctahedral character in the phyllosilicates. Groupings in the analyses, combined with XRD data, allow the specific compositions of each of the mafic phyllosilicate types to be identified.

The presence of random and several types of regular mixed-layer chlorite/smectite as well as chlorite suggests that the transition between these minerals may occur in the form of a continuous variation in the proportion of mixed-layer content rather than in a series of jumps, which has also been proposed.

Variations in the compositions of the mafic phyllosilicates in this sequence are reflected by a wide divergence from the ideal clinochlore end-member. However, it is this ideal mineral that is generally used as an excess phase and projection point for modeled systems at low grades of metamorphism. Calculated clinochlore activities for the samples studied show a range from 0.005 to 0.070, which is as wide as the 1σ range reported by Frey et al. (1991) for chlorite in low-grade metamorphic areas from 19 different literature sources. Such variation in chlorite composition is one of the causes of considerable overlap of the various subgreenschist facies reported by Frey et al. (1991) and also a cause of the difficulty in assigning a facies to low-grade sequences such as that reported here.

Introduction

Mafic phyllosilicates are ubiquitous minerals in very low-grade and low-grade metamorphosed basic igneous rocks. Detailed accounts of such minerals in hydrothermally metamorphosed basalts in a transition from the zeolite to lower greenschist facies in Iceland have been presented by Kristmansdóttir (1975, 1979) and more recently by Schiffman and Fridleifsson (1991). Shau and Peacor (1992) have studied such minerals in altered basalts from DSDP Hole 504B. Similar studies have also been undertaken on mafic phyllosilicates in the hydrothermally altered Point Sal Ophiolite (Bettison and Schiffman, 1988). These investigations have established that the mafic phyllosilicates are diverse in chemical and structural character. X-ray diffraction and electron microprobe analysis have shown that the minerals vary from smectite to random mixed-layer chlorite/smectite in the zeolite facies, with chlorite only becoming dominant in the greenschist facies.

In contrast, however, the nature of the mafic phyllosilicates in low-grade regionally metamorphosed basalts is little studied. In an investigation of a zeolite through prehnite pumpellyite to greenschist facies transition in metabasites from the Karmutsen area, Cho et al. (1986) and Cho and Liou (1987) reported, on the basis of microprobe data alone, that the mafic phyllosilicate phase was chlorite of a relatively restricted composition, ranging between pycnochlorite and diabanite. It is often the case that chlorite in such low-grade rocks is identified on the basis of microprobe analyses alone, with little or no XRD data being reported. Most recently, however, a detailed investigation of the character of mafic phyllosilicates in a regionally metamorphosed basalt from northern Taiwan (Shau et al., 1990), using TEM/AEM, EMPA,

0003–004X/93/0304–0377$02.00

XRD, and optics, indicated the occurrence of corrensite and mixed-layer chlorite/corrensite.

Studies relating to phyllosilicate character in low-grade metabasites have implications for the proposed model systems in such rocks (CASH and NCMASH, Liou et al., 1985; Frey et al., 1991). In these systems chlorite, usually of a constant clinochlore composition, is used as a projection point.

As the data available on the most dominant phase in low-grade regional metabasites are so limited, it is one of the aims of this study to determine the character of the mafic phyllosilicates by combined optical, XRD, and EMPA means. The results presented emphasize some of the difficulties of identifying mafic phyllosilicates on the basis of limited optical and microprobe data. In addition, the assumption of a constant chlorite composition when applying model systems is assessed.

Geological setting

Samples are from a succession of low grade metabasalts of late Proterozoic age from eastern North Greenland, 1300 m thick, known as the Zig-Zag Dal Basalt Formation (Jepsen et al., 1980; Kalsbeek and Jepsen, 1984). In the type section at Zig-Zag Dal some 40 individual flows are exposed, which typically show highly vesicular and sometimes brecciated tops. Many flows possess well-developed columnar jointing.

Metamorphic assemblages in these metabasites variably contain albite, prehnite, pumpellyite, calcite, white mica, titanite, and rare zeolite, along with ubiquitous mafic phyllosilicates (Bevins et al., 1992). Rarely are low variance assemblages present; instead, secondary minerals are scattered throughout individual rock thin sections or form mono- or bimineralic assemblages in vesicles, and more than one mafic phyllosilicate may be present within individual assemblages. Such high-variance assemblages are of limited value in determining metamorphic facies. However, the presence or absence of various minerals is of significance, in particular the absence of epidote, which implies that temperatures in the sequence did not greatly exceed 200 °C (Cho et al., 1986). Above 200 °C, epidote is thought to appear as a result of the discontinuous reaction laumontite + pumpellyite = epidote + chlorite + quartz + H_2O, a reaction that Cho et al. (1986) considered to represent the transition from the zeolite to the prehnite pumpellyite facies. The inference is, therefore, that despite the paucity of zeolites and relative abundance of prehnite and pumpellyite, the metamorphism is at zeolite to lowermost prehnite pumpellyite facies (Bevins et al., 1992).

It is relevant to emphasize that, as detailed by Bevins et al. (1992), alteration is variable both between flows and within flows. Whereas vesicular and brecciated flow margins typically show higher degrees of alteration (reflected in the modal proportions of secondary minerals), no systematic increase in alteration is seen with depth. In addition, flows in the Zig-Zag Dal sequence showing only very low alteration states occur sandwiched between highly altered flows. A most pronounced difference between relatively altered and relatively fresh flows is readily observed in the field in the form of color differences; the more altered flows show a strong green coloration, whereas the fresher flows show an orange hue, which reflects the variation in the type of mafic phyllosilicate present in the flows.

Analytical methods

All samples utilized in this study are from the collections of the Geological Survey of Greenland and are preceded by the numbers 273 (e.g., 273471). Eight samples were selected for detailed analysis of the mafic phyllosilicates, and some 150 microprobe spot analyses were obtained. The mineral analyses were obtained using a Cameca Camebax electron microprobe at the Department of Geology, University of Manchester. The operating conditions were 15 kV and 3.5×10^{-8} A, with a spot size of ca. 3 μm. Calibration was against metals, oxides, and silicates.

For X-ray diffraction studies, small chips of the basalt were ultrasonically treated to separate the phyllosilicates from the rock matrix. A <2-μm fraction was separated by centrifuge and vacuum filtration methods. Samples were glycol solvated at 60 °C for at least 12 h and heated for 1 h. A Philips PW1800 diffractometer with Cu$K\alpha$ radiation, operated at 40 kV and 50 mA and with automatic divergence slit and graphite monochromator, was used.

Phyllosilicate characteristics

Petrography

Four types of mafic phyllosilicates are abundant in the Zig-Zag Dal metabasalts, occurring as pseudomorphs after mafic minerals (most typically olivine) in the groundmass of lavas and as vesicle infills. In plane light, three of the four types have a strong green color, whereas the fourth is brown to orange-brown. The various phyllosilicates correlate closely with the intensity of rock alteration. In the least-altered parts of flows (in which primary calcic plagioclase is preserved and secondary calc-silicates are absent) the orange-brown mafic phyllosilicate predominates. This phase generally lacks pleochroism and has moderately high birefringence, although this is typically masked by strong body colors. In other studies, phyllosilicates with these optical properties have been identified as having a high smectite component, and XRD and microprobe evidence presented below shows that these phyllosilicates are random mixed-layer chlorite/smectite.

In the moderately to strongly altered flows and parts of flows, where primary plagioclase is replaced by albite, and various secondary calc-silicate minerals may also be present, the mafic phyllosilicates are green in color. These are only weakly pleochroic (light to dark green) and show low (anomalous) birefringence; this phyllosilicate type is shown below to be chlorite. In contrast, however, in a

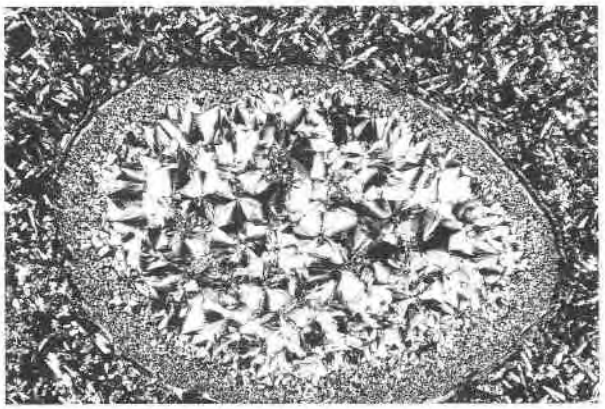

Fig. 1. Photomicrograph of mafic phyllosilicates in sample 455, identified as a regular mixed-layer chlorite/smectite in matrix and as rim to vesicle and discrete chlorite in vesicle infilling. Vesicle long axis is 4 mm.

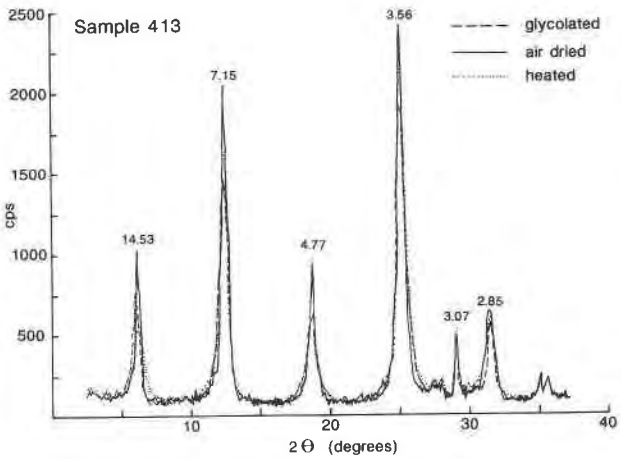

Fig. 2. XRD patterns of sample 413 for air-dried state, glycolated and heated to 315 °C. The almost total overlap between the different profiles is indicative of a discrete chlorite with a minimum (<10%) of mixed layering.

few samples, phyllosilicates similar to those above but showing slightly higher birefringence (to upper first order) are present, which are identified below as regular mixed-layer chlorite/smectite. The third type of green phyllosilicate occurs only in a small number of flows and shows an emerald-green color in plane light and moderate birefringence. These distinctive features accord with XRD and microprobe data, which indicate that this is celadonite.

As mentioned above, more than one phyllosilicate may occur within individual samples. Celadonite, for example, typically occurs in association with chlorite, whereas regular mixed-layer chlorite/smectite is sometimes found with chlorite. In sample 455, coarse discrete chlorite infills vesicle centers, whereas regular mixed-layer chlorite/smectite (with higher birefringence) forms the main alteration phase in the groundmass, as a rim to vesicles, as seen in Figure 1. The optical character of these phases, however, bears a strong resemblance to the yellowish-green platy corrensite lining vesicles cored by a pale green phase identified as a mixed-layer chlorite/corrensite by Shau et al. (1990) in metabasalts from northern Taiwan. In one sample (471), a similar relationship is found between random mixed-layer chlorite/smectite and chlorite. In some cases the contacts between different types of coexisting mafic phyllosilicates are hard to distinguish, and the optical properties are suggestive of physical intergrowth of the two phases.

XRD results

In the following sections the samples are treated on the basis of the differing phyllosilicate assemblages recognized through XRD patterns.

Chlorite. Three samples (413, 426, and 447) have a single mafic phyllosilicate, which shows optical properties characteristic of true chlorite. The XRD patterns of air-dried, glycolated, and heated material from sample 413 are representative of this group and are shown in Figure 2. Glycolation and heating result in only the slightest of changes in the peak positions and shape, the most noticeable being a slight increase in the asymmetry of the 002 and 004 peaks and a broadening of the 003 peak on both the high and low 2θ sides. These changes are in accordance with the presence of a small mixed-layer content, as detailed later for sample 455. Using the Hower (1981) migration curves, the smectite content is estimated as 13 and 8% with the 001 and 002 peaks, respectively. However, the 002 reflection is regarded as the more reliable (Hower, 1981), and here such phases with <10% mixed layering are regarded as pure chlorite. In the case of samples 426 and 447, the chlorite percentages calculated from the 002 peak positions are also high, being 95 and 93%, respectively. Other low-intensity peaks in the pattern (Fig. 2) are indicative of the presence of calcite, feldspar, and hematite(?).

Chlorite and celadonite. Samples 437 and 467 also contain chlorite, their XRD patterns being similar to that of sample 413 (Fig. 2), with periodic reflections up to 005. Similar slight asymmetrical expansion of the 001 and 002 peaks occurs on glycolation, again suggestive of only a small mixed-layer content of <10%. The chlorite contents derived from the 002 peak positions for samples 437 and 467 are both 96%. These XRD patterns additionally contain an integral series of peaks at 10.1, 4.99, and 3.31 Å, which is representative of celadonite. The 001 celadonite peak also shows a slight change in the peak shape on glycolation, but the higher order peaks are not affected, and so any mixed-layer component is considered to be small. The patterns also show peaks indicative of feldspar and hematite(?).

Chlorite and regular mixed-layer chlorite/smectite. Three samples (415, 444, 455), shown petrographically to have chlorite and a second mafic phyllosilicate with green colors but higher birefringence, have noticeably different XRD patterns. In Figure 3 the glycolated pattern

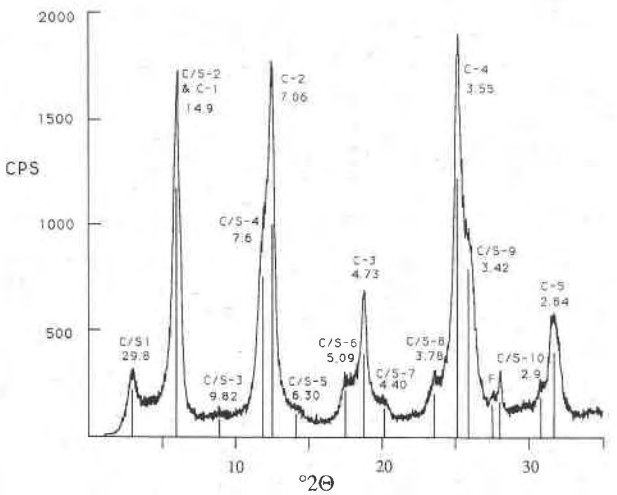

Fig. 3. XRD glycolated pattern for sample 455. Peaks C-1, C-2, etc. refer to a chlorite 001, 002, etc. rational series; C/S-1, C/S-2, etc. to regular mixed-layer chlorite/smectite (65:35) (see text) with 001, 002 reflections, etc.

for sample 455 is shown, which is representative of this group. A superlattice peak is developed at 29.8 Å, and the peaks above 10° 2θ become markedly asymmetrical, some to the low-angle (e.g., 7-Å peak), and others to the high-angle (e.g., 3.55-Å peak) sides. This asymmetry is caused by the overlap of reflections from discrete chlorite and regular mixed-layer chlorite/smectite, as detailed below.

The presence of discrete chlorite is recognized by a rational series of peaks in the glycolated patterns at 7.06, 4.73, 3.55, and 2.84 Å, the positions of which represent the peak maxima (Fig. 3). The peak at 14.9 Å is not sufficiently resolved to identify the discrete chlorite. Using the Hower (1981) migration curves for the 002 peak indicates the chlorite contents for samples 415 and 455 to be 100% and 97% for sample 444.

The overlap of the discrete chlorite peaks with the mixed-layer peaks makes the identification of the exact mixed-layer peak positions more difficult. The most readily discernible peak resulting from the mixed-layer mineral, apart from the superlattice peak, is that occurring at the 5.09-Å position (Fig. 3). If this peak position is taken as the 006 reflection of the mixed-layer mineral and is used to calculate a rational series of reflections, then the values generated are very close to those identified using the APD software. These peak positions are shown in Figure 3 and represent a very good fit to the shoulders of the discrete chlorite peaks, thus explaining satisfactorily the peak asymmetries seen in the full pattern. Using the eight peak positions determined by the APD software (003–00,10) the coefficient of variability (Bailey, 1982) is 0.70%. Values of <0.50% are normally taken to identify an $R1$ ordering and a 50:50 proportion of components. Thus, although this mineral has a high degree of regularity it cannot be considered as true corrensite. The coefficient of variability calculated for sample 415 is 0.39% (Robinson and Bevins, in preparation), and so in that case the mineral can be regarded as true corrensite.

Determination of the smectite content in the regular mixed-layer chlorite/smectite in this sample using the method of Hower (1981) gives 35% with the 004 (31 Å)/002 (17 or 14 Å) peak combination, which has $d = 7.64$ Å. According to Hower (1981), this peak combination is more reliable than the 15-Å peak combination because of variation caused by crystallite size difference. This smectite content is in accord with the lower coefficient of variability measured, indicating a departure from the ideal 50:50 proportions for such a structure.

The XRD pattern for a $R1$, chlorite/smectite (glycol) structure in 65:35 proportions has been modeled using the Newmod program (Reynolds, 1985) and is shown in Figure 4a. Mixed-layer chlorite/smectite with these relative proportions of the two components gives 006 and 008 reflections that accord closely with the determined values for sample 455, as shown in Figures 3 and 4a. These two peaks are the most readily measured on the diffraction pattern because of the lack of overlap with adjacent chlorite peaks. The matching of the 006, 008, and 009 reflections between the modeled and observed patterns is at the same proportion of chlorite (0.65) as determined by the migration curves of Hower (1981) on the natural sample. Reducing the chlorite component to 0.6 results in migration of these peaks to higher d values than those observed, whereas an increase to 0.7 results in a major reduction in the intensity of the superlattice peak and migration of the above peaks to lower d values than observed. The absence of a 003 peak (ca. 10 Å) in the calculated pattern is indicative of low-charge corrensite (Bailey, 1988); however, a very low-intensity 9.82-Å peak is present in the measured pattern, and that suggests that some of the layers may be of a high-charge corrensitic character (vermiculite). Also, the relatively low intensity of the 001 peak (29.8 Å) is also indicative of a greater chlorite content than the ideal 50:50 proportions for corrensite.

An XRD pattern for a physical mixture of discrete chlorite and regular mixed-layer chlorite/smectite (of the same character as that in Fig. 3) in the respective proportions 55:45, calculated using the Newmod program, is shown in Figure 4b. The pattern closely resembles that of the observed scan shown in Figure 3; the major difference is in the greater resolution of the overlapping peaks for the composite 7- and 5-Å peaks and the relatively low intensity of the superlattice peak in the calculated profile. Decreasing the chlorite proportion to 50% results in a splitting of the 3.55-Å peak, whereas decreasing the chlorite/smectite content makes the shoulder on the 3.55-Å peak become very much less noticeable. Thus the chlorite to chlorite/smectite proportions of 55:45 appear to give a realistic measure of the two discrete phases in this sample.

Although the observed and calculated patterns (Figs. 3, 4b) represent quite a good match, the anomalies itemized

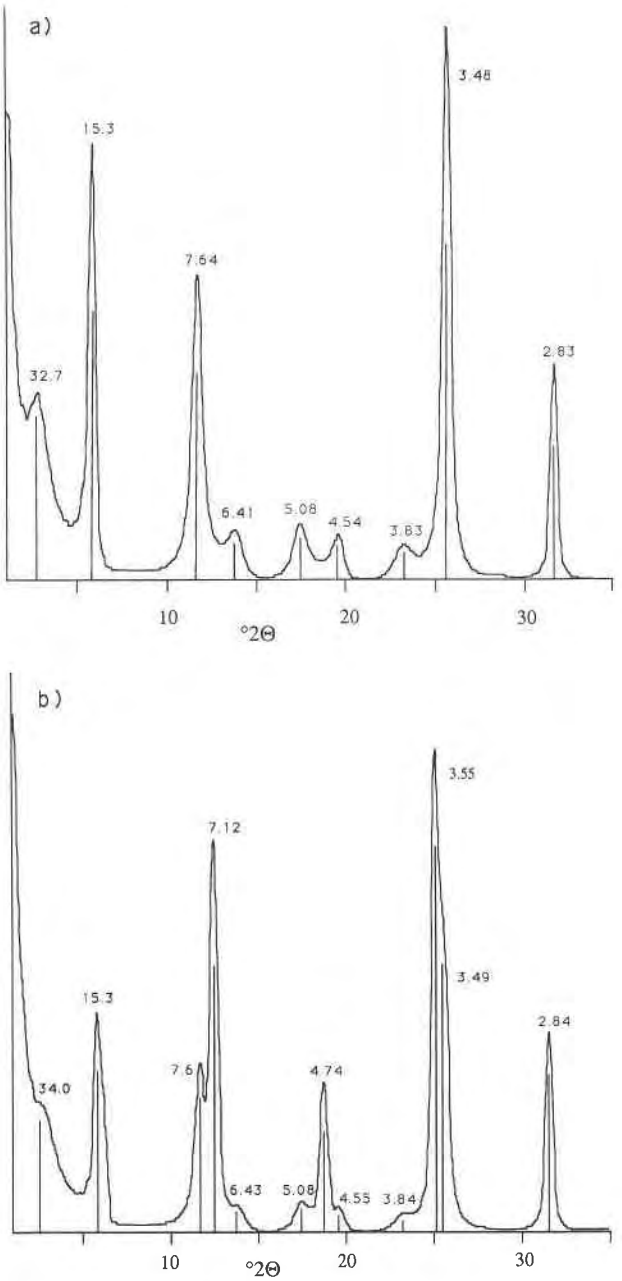

Fig. 4. Calculated glycolated XRD patterns for chlorite/smectite (65:35) and chlorite (Reynolds, 1985). (**a**) Pattern for a regular mixed-layer tri-chlorite/tri-smectite 2-glycol with 65% chlorite content. (**b**) Pattern for a physical mixture between a discrete tri-chlorite and a tri-chlorite/tri-smectite 2-glycol mixed-layer mineral in the respective abundances of 55 and 45%, with the proportion of chlorite in the mixed-layer mineral at 65%.

above suggest that there may be an additional mineral with peaks lying between those of the chlorite and the recognized regular chlorite/smectite (65:35), and thus causing the less well-resolved peaks in the observed profile. Robinson and Bevins (in preparation) have undertaken a detailed analysis of this feature in the case of

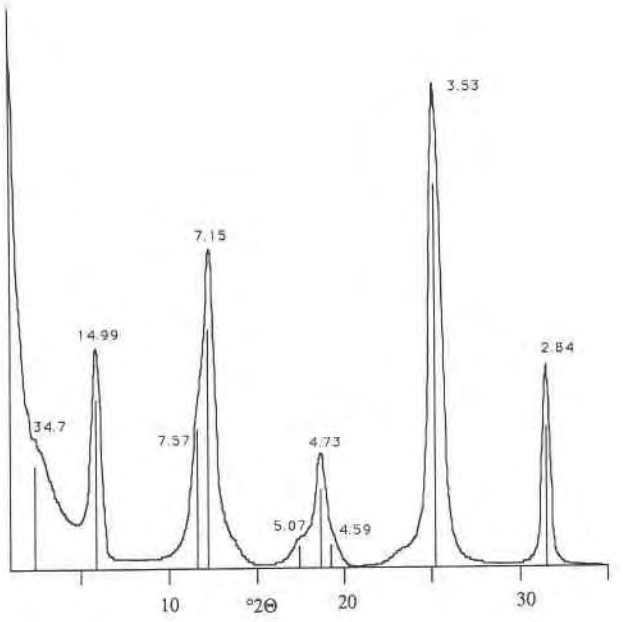

Fig. 5. Newmod-calculated XRD pattern for a physical mixture among a discrete tri-chlorite, a tri-chlorite/tri-smectite (65:35) 2-glycol mixed-layer, and a tri-chlorite/tri-smectite (85:15) 2-glycol mixed-layer, in the respective abundances of 25, 25, and 50%.

sample 415, which shows similar anomalies between the calculated and observed profiles to that of sample 455. Their analysis involved peak fitting to the various composite diffraction peaks, utilizing a deconvolution approach. This showed that a mixture of two minerals, chlorite and a regular chlorite/smectite (60:40), resulted in a poor match between the fitted and observed profiles. Profiling on the basis of an additional variety of regular chlorite/smectite (80:20) in the mixture, however, resulted in a near-perfect match between the fitted and observed profiles.

Similar treatment for sample 455 suggests that an additional variety of regular chlorite/smectite (85:15) is also present. A Newmod-modeled XRD pattern for a mixture of chlorite, chlorite/smectite (65:35), and chlorite/smectite (85:15) in proportions 25:25:50 is shown in Figure 5. This mixture shows a closer resemblance to the observed pattern in that the less well-resolved composite peaks at 7 and 5 Å in the observed pattern are now matched to a high degree.

Sample 444 also has an XRD pattern similar to those of samples 415 and 455, but the overall peak intensities are much weaker, and the asymmetries due to the regular chlorite/smectite component are accordingly more difficult to resolve. The chlorite proportion calculated from the Hower curves as above is also 65% for the 7-Å peak. In addition, weak peaks at 9.93 and 3.32 Å confirm the presence of celadonite, recognized petrographically.

Chlorite and random mixed-layer chlorite/smectite. Sample 471 has two phyllosilicates, a discrete chlorite and an orange-brown mafic phyllosilicate. Although the

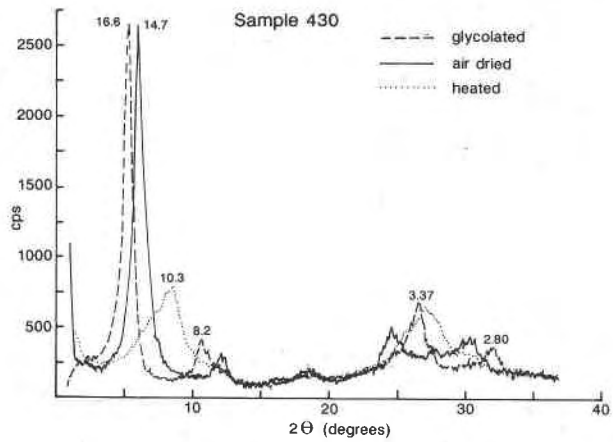

Fig. 6. XRD patterns for sample 430, for air-dried state, glycolated, and heated to 315 °C. The pattern is representative of a virtual monomineralic random mixed-layer chlorite/smectite (25:75).

XRD peak intensities were low, the pattern consists of a normal chlorite diffraction pattern and a set of peaks that is identical to those described below for random mixed-layer chlorite/smectite.

Random mixed-layer chlorite/smectite. In samples 430 and 464, the only phyllosilicate is an orange-brown phase. The XRD patterns obtained on material from sample 430 are shown in Figure 6; the basal reflection expands from 14.7 Å in the air-dried state to 16.6 Å on glycolation, but no superlattice peak is evident. Heating to 325 °C causes collapse of the smectitic component of the structure, to give a basal peak with a maximum peak height around 10.3 Å, but centered around 11 Å. The presence of smaller peaks in the pattern of the heated material at 7.1, 4.8, and 3.6 Å is indicative of a chlorite component. These patterns represent monomineralic random mixed-layer chlorite/smectite. From the position of the 002 peak the chlorite concentration is calculated as 25% from the migration curves of both Hower (1981) and Reynolds (1988).

The glycolated pattern (Fig. 6) is virtually identical to the calculated pattern for a randomly interstratified chlorite/smectite with 25% chlorite, as given by Reynolds (1988). The glycolated profile of sample 430, with its 3.37-Å peak of greater intensity than the 8.2 Å, the extremely low intensity of the 5.5-Å peak, and the absence of a 4.3-Å peak, is indicative of the trioctahedral character of the chlorite and smectite components (Reynolds, 1988).

Chemistry

All electron microprobe phyllosilicate analyses have been recalculated on the basis of a chlorite formula with 28 O atoms from which the following chemical parameters are derived; noninterlayer cations (Si + Al + Fe + Mg + Mn); interlayer cations (Ca + Na + K); and chlorite content (x) in mixed-layer chlorite/smectite. An x value of unity represents the chlorite end-member (trioctahedral) having a total of 20 noninterlayer cations, compared with the end-member smectite ($x = 0$), which on the basis of the chlorite formula with 28 O atoms would have a total of 17.82 noninterlayer cations. The proportion of chlorite layers (x) is determined by extrapolation between these two end-members, as based on individual

Table 1. Mean compositions (wt%) and 1σ values for mafic phyllosilicates from the Zig-Zag Dal Basalt Formation

Sample	430(9) Ran C/S		464(3) Ran C/S		471(8) Ran C/S		415(7) C/S1 (60:40)		415(14) C/S2 (80:20)		455(5) C/S2 (65:35)		455(9) C/S1 (85:15)		413(8)-Chl	
SiO_2	41.20	0.75	40.26	0.74	40.63	0.96	33.72	0.51	32.93	1.02	32.37	0.24	30.38	0.61	31.38	0.68
TiO_2	0.04	0.06	0.03	0.05	0.00	0.00	0.00	0.00	0.00	0.00	0.00	0.00	0.00	0.00	0.01	0.02
Al_2O_3	9.93	0.46	10.22	0.65	10.45	0.23	13.79	0.18	14.19	0.46	13.66	0.26	14.23	0.54	15.96	0.98
FeO	20.86	0.36	21.95	0.74	19.79	1.01	18.43	0.59	18.75	0.56	23.91	0.17	26.30	1.49	23.57	0.67
MnO	0.12	0.08	0.06	0.08	0.03	0.08	0.46	0.10	0.77	0.35	0.30	0.06	0.36	0.07	0.37	0.11
MgO	15.00	0.37	14.85	0.07	15.47	0.26	19.02	0.56	19.07	0.42	15.15	0.20	14.29	0.75	16.81	0.84
CaO	2.69	0.16	2.42	0.15	2.93	0.28	0.81	0.10	0.69	0.17	1.29	0.05	0.98	0.19	0.84	0.12
Na_2O	0.09	0.15	0.22	0.36	0.04	0.11	0.00	0.00	0.00	0.00	0.13	0.17	0.12	0.15	0.16	0.10
K_2O	0.16	0.06	0.08	0.05	0.21	0.16	0.13	0.10	0.08	0.09	0.00	0.00	0.00	0.00	0.04	0.04
TOTAL	90.09		90.09		89.55		86.36		86.48		86.81		86.66		89.14	
Si	8.07	0.12	7.94	0.15	7.97	0.14	6.90	0.03	6.75	0.16	6.80	0.03	6.51	0.08	6.41	0.08
Ti	0.01	0.01	0.00	0.01	0.00	0.00	0.00	0.00	0.00	0.00	0.00	0.00	0.00	0.00	0.00	0.00
$^{[4]}Al$	0.00	0.05	0.06	0.12	0.03	0.09	1.10	0.03	1.25	0.16	1.20	0.03	1.49	0.08	1.59	0.08
$^{[6]}Al$	2.29	0.05	2.31	0.11	2.39	0.05	2.22	0.03	2.19	0.04	2.19	0.02	2.10	0.08	2.25	0.08
Fe_2	3.42	0.07	3.62	0.11	3.25	0.18	3.15	0.13	3.22	0.12	4.20	0.04	4.71	0.32	4.02	0.16
Mn	0.02	0.01	0.01	0.01	0.00	0.01	0.08	0.02	0.13	0.06	0.05	0.01	0.07	0.01	0.06	0.02
Mg	4.38	0.10	4.36	0.05	4.52	0.10	5.80	0.12	5.83	0.09	4.75	0.03	4.56	0.20	5.11	0.14
Ca	0.56	0.03	0.51	0.03	0.62	0.06	0.18	0.02	0.15	0.04	0.29	0.01	0.22	0.04	0.18	0.03
Na	0.03	0.06	0.08	0.14	0.02	0.04	0.00	0.00	0.00	0.00	0.05	0.07	0.05	0.06	0.06	0.04
K	0.04	0.02	0.02	0.01	0.05	0.04	0.03	0.03	0.02	0.02	0.00	0.00	0.00	0.00	0.01	0.01
x	0.13		0.19		0.13		0.60		0.66		0.57		0.70		0.70	
Fe/(Fe + Mg)	0.44		0.45		0.42		0.35		0.36		0.47		0.51		0.44	

Note: Values in parentheses refer to number of analyses used to calculate the mean. Ran C/S = random mixed-layer chlorite/smectite; C/S1, C/S2 = types of regular mixed-layer chlorite/smectite; Chl = discrete chlorite; Ce = celadonite; sample 444 contains regular mixed-layer chlorite/smectite whose compositions are not able to be satisfactorily distinguished; x = chlorite content in mixed-layer chlorite/smectite determined by recalculation of microprobe analyses, as detailed in text.

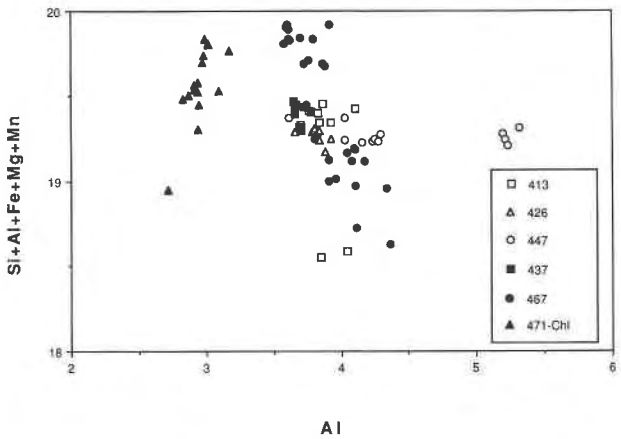

Fig. 7. Noninterlayer (Si + Al + Fe + Mg + Mn) cation total vs. Al_{tot} for samples with only chlorite (samples 413, 426, and 447 = open symbols); chlorite + second phyllosilicate phase (closed symbols), which include chlorite + celadonite (samples 437 and 467), and chlorite + random mixed-layer chlorite/smectite (sample 471-Chl). This figure and all subsequent figures show analyses plotted on the basis of a chlorite formula with 28(O,OH).

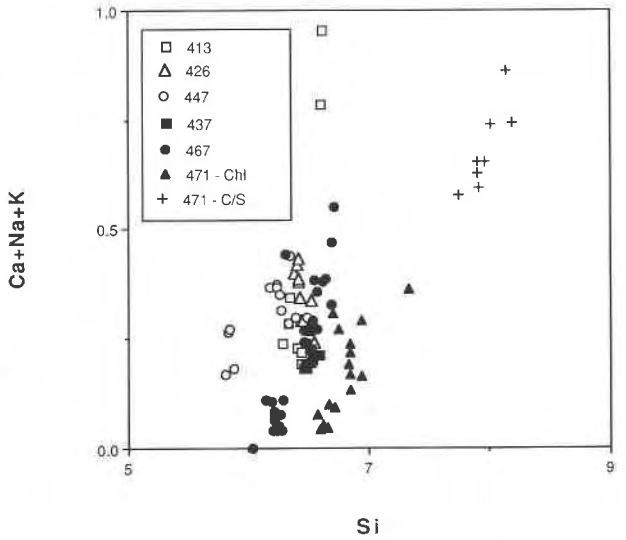

Fig. 8. Interlayer cation (Ca + Na + K) totals vs. Si contents for samples with ornamentation as given for Fig. 7.

microprobe analyses (Schiffman and Fridleifsson, 1991). Averaged results and standard deviations for the analyzed phyllosilicates are presented in Table 1.

Considerable diversity in the composition of the phyllosilicates in the studied samples has been observed; these variations are considered below in terms of the phyllosilicate assemblages present in individual samples.

Chlorite. Chlorite was identified, on the basis of XRD characteristics, as the only phyllosilicate in three samples (413, 426, and 447) for which 33 analyses are available. All of these analyses show similar characteristics, with the exception of two points for sample 413, which have higher interlayer contents, and four points for sample 447, which show higher Al_{tot} contents. Ignoring these, the noninterlayer cations total in the range 19.3–19.5 (Fig. 7), interlayer cations are <0.42 (Fig. 8), and x values are between 0.60 and 0.73.

TABLE 1. *Continued*

415(3)-Chl		426(10)-Chl		437(8)-Chl		444(7)		447(13)-Chl		455(7)-Chl		467(13)-Chl		471(6)-Chl		467(13)-Ce	
31.43	0.07	29.94	0.52	31.53	0.47	32.85	1.85	29.49	0.97	27.87	0.76	28.99	0.47	30.96	0.28	52.47	1.85
0.00	0.00	0.02	0.03	0.02	0.06	0.00	0.00	0.05	0.05	0.00	0.00	0.00	0.00	0.00	0.00	0.00	0.00
14.73	0.12	15.05	0.41	15.17	0.34	14.06	0.48	18.01	2.54	15.24	1.06	14.71	0.74	11.98	0.28	14.14	3.35
19.28	0.23	31.42	0.45	21.77	0.30	23.24	2.41	26.27	1.48	30.31	2.31	27.79	3.14	30.18	0.79	13.62	3.49
1.13	0.08	0.53	0.07	0.24	0.15	0.25	0.32	0.26	0.12	0.34	0.22	0.31	0.19	0.04	0.09	0.00	0.00
18.94	0.06	10.45	0.31	17.68	0.32	15.36	0.51	13.16	0.53	12.34	1.05	15.33	1.90	14.69	0.27	4.85	1.38
0.47	0.04	0.91	0.07	0.84	0.12	0.76	0.23	1.11	0.25	0.25	0.18	0.26	0.13	0.30	0.10	0.37	0.26
0.00	0.00	0.28	0.13	0.00	0.00	0.08	0.14	0.13	0.09	0.00	0.00	0.00	0.00	0.00	0.00	0.10	0.14
0.04	0.05	0.09	0.11	0.07	0.08	0.81	0.72	0.01	0.02	0.00	0.00	0.00	0.00	0.00	0.00	8.64	0.61
86.02		88.69		87.32		87.41		88.49		86.35		87.39		88.15		94.19	
6.53	0.03	6.44	0.05	6.51	0.04	6.84	0.29	6.16	0.24	6.15	0.16	6.21	0.06	6.64	0.05	7.47	0.27
0.00	0.00	0.00	0.01	0.00	0.01	0.00	0.00	0.01	0.01	0.00	0.00	0.00	0.00	0.00	0.00	0.00	0.00
1.47	0.03	1.56	0.05	1.49	0.04	1.16	0.29	1.84	0.24	1.85	0.16	1.79	0.06	1.36	0.05	0.53	0.27
2.14	0.02	2.26	0.07	2.20	0.05	2.29	0.27	2.60	0.36	2.11	0.12	1.93	0.10	1.67	0.05	1.84	0.34
3.35	0.03	5.65	0.11	3.76	0.08	4.05	0.47	4.59	0.28	5.59	0.42	4.98	0.62	5.41	0.11	1.62	0.45
0.20	0.01	0.10	0.01	0.04	0.03	0.04	0.06	0.05	0.02	0.06	0.04	0.06	0.03	0.01	0.02	0.00	0.00
5.87	0.01	3.35	0.08	5.44	0.07	4.77	0.20	4.10	0.17	4.06	0.34	4.90	0.51	4.69	0.08	1.03	0.29
0.10	0.01	0.21	0.02	0.19	0.03	0.17	0.05	0.25	0.06	0.06	0.04	0.06	0.03	0.07	0.02	0.06	0.04
0.00	0.00	0.12	0.06	0.00	0.00	0.03	0.05	0.05	0.04	0.00	0.00	0.00	0.00	0.00	0.00	0.03	0.04
0.01	0.01	0.02	0.03	0.02	0.02	0.22	0.19	0.00	0.01	0.00	0.00	0.00	0.00	0.00	0.00	1.57	0.10
0.75		0.66		0.70		0.55		0.64		0.89		0.92		0.87			
0.36		0.63		0.41		0.46		0.53		0.58		0.50		0.54		0.61	

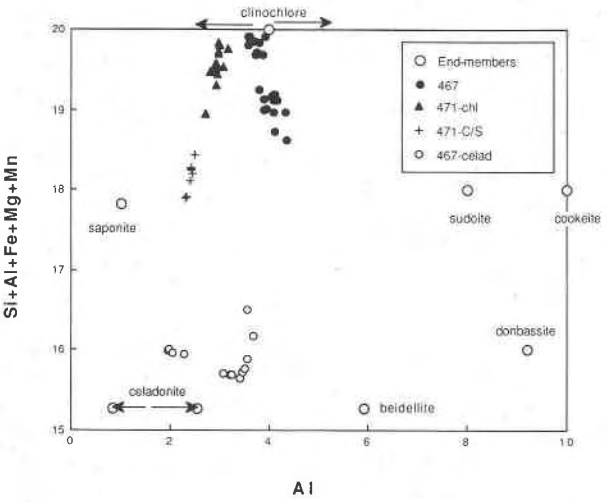

Fig. 9. Noninterlayer cations vs. Al_{tot} content for mafic phyllosilicates and celadonite in samples 467 and 471. Labeled large circles for mafic phyllosilicates are end-member compositions taken from Bailey (1988) and for celadonite from Buckley et al. (1978); arrows for clinochlore and celadonite show general ranges of composition.

The two of the ten analyses of sample 413 that plot well away from the main group (Figs. 7, 8) have high Ca + Na + K contents reflecting their low x values, which is caused by high CaO contents (>3 wt%). The XRD pattern for this sample contains peaks for calcite, and, as discussed earlier, the chlorite profile suggests that a minimum of mixed-layering is present. It would thus appear that the high CaO does not occur in chlorite but is representative of a physical mixture between calcite and chlorite leading to analytical contamination.

Chlorite in samples 426 and 447 has compositions very similar to that in sample 413, with consistent values for noninterlayer (Fig. 7) and interlayer cation (Fig. 8) totals and x values. Sample 447, although showing a clustering in terms of noninterlayer and interlayer totals and x values, has four analyses with markedly higher Al_{tot} contents (>5 atoms pfu) and tetrahedral contents (>2 atoms pfu) compared with the lower values in sample 447 and in samples 413 and 426 (Fig. 7).

For these three samples, however, the XRD patterns suggest that there is <10% of mixed-layering present, which contrasts markedly with the much lower mean chlorite contents (x values) of 0.70, 0.66, and 0.64, recalculated from the microprobe analyses, for samples 413 (anomalous 2 points omitted), 426 and 447, respectively.

Chlorite and celadonite. Samples 437 and 467 also contain discrete chlorite but in addition have variable amounts of celadonite. Chlorite analyses in sample 437 show a close grouping and have a similar chemical character to chlorite in the previous assemblage (Figs. 7, 8). Analyses of chlorite in sample 467, however, are unlike those of the previous four samples in that they show a much greater spread in noninterlayer (Fig. 7) and interlayer cation totals (Fig. 8) and x values.

In sample 467, two distinct populations of analyses can be discerned. The first population has 13 of the 26 analyses with noninterlayer cation totals >19.7 (Fig. 7), a very close clustering in interlayer cation totals of ca. <0.1 (Fig. 8), and x values >0.8. These analyses lie near the ideal chlorite compositional range, as indicated by the trichlorite point (clinochlore) in Figure 9. The second set of 13 analyses shows a near vertical trend in noninterlayer cation totals, which are much lower than the first group, ranging from 18.5 to 19.3 (Fig. 7), and interlayer cation totals are >0.1. However, the range of interlayer cation totals in this second set is generally similar to that seen in samples whose XRD patterns are indicative of the presence of chlorite only (samples 413, 426, and 447; Fig. 8). In all samples for which data are plotted in Figure 8 with interlayer cations >0.10, the dominant interlayer cation is Ca, with values between 0.15 and 0.25. Although Ca remains dominant in the second set of analyses from sample 467, there is a much higher content of K, as shown by the mean value of 0.12 (1σ = 0.09), in contrast to the other samples shown in Figure 9, where the K content is <0.02.

Microprobe analyses of celadonite in this sample are recalculated on the basis of the chlorite formula and shown in Figure 9 along with those of the chlorite. The celadonite analyses from sample 467 (smaller open circles) lie close to the ideal formula range of celadonite, as given by Buckley et al. (1978), which are shown as larger open circles in Figure 9.

Chlorite and random mixed-layer chlorite/smectite. In sample 471, discrete chlorite as well as an orange-brown phyllosilicate are present. Sixteen analyses of chlorite are shown on Figure 7 (closed triangles), which define a linear trend in noninterlayer values with a range from 19.3 to 19.9 (excepting one anomalously low value of 18.95). Interlayer cation totals are typically <0.3 (Fig. 7). On Figures 8 and 9, eight analyses of the orange-brown phyllosilicate (sample 471-C/S) coexisting with the chlorite are shown, clearly demonstrating their markedly higher interlayer cation totals (0.5–0.9), and lower noninterlayer cation totals (17.9–18.4). This phase also has higher SiO_2 and lower Al_2O_3 contents than either discrete chlorite or regular mixed-layer chlorite/smectite.

The range of analyses for the two phases in sample 471 (Fig. 9, 471-Chl and 471-C/S) shows a trend from near-ideal chlorite composition with 20 noninterlayer cations toward the point representative of the ideal trioctahedral smectite (saponite), with 17.8 noninterlayer cations. There is, however, a marked dichotomy between the chlorite-like and saponite-like analyses in this sample, apart from one of the chlorite group of analyses with a high CaO content (triangle of <19, Fig. 9). This dichotomy is supported by the XRD pattern of this sample, which, although of low intensity, indicates the presence of two discrete phases rather than a continuum between the end-members of chlorite and saponite.

Chlorite and regular mixed-layer chlorite/smectite. XRD data for samples 415, 444, and 455 show that they

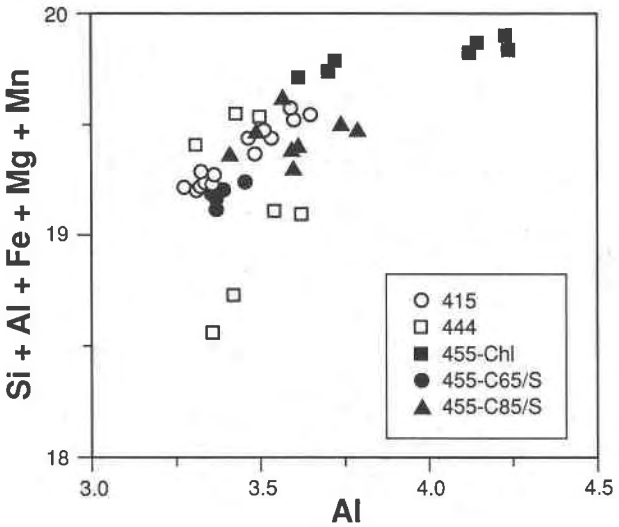

Fig. 10. Noninterlayer cation total vs. Al_{tot} for samples (415, 444, and 455) with discrete chlorite and regular mixed-layer chlorite/smectite. Analyses for 455 split into those from vesicle-filling chlorite (squares), matrix and vesicle rim (circles), and mixed regions near vesicle rim (triangles).

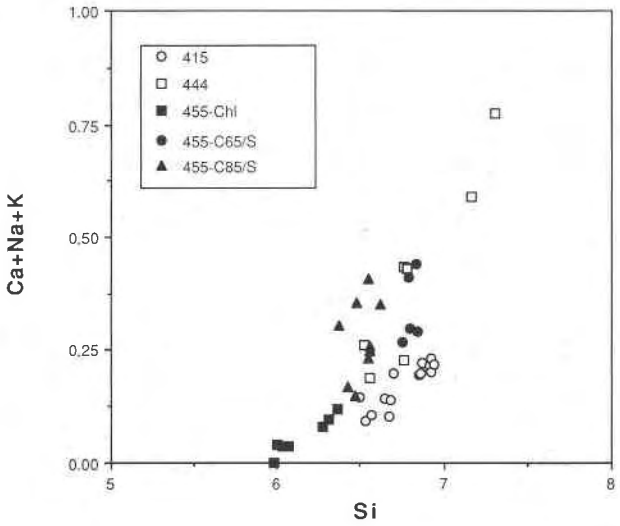

Fig. 11. Interlayer cation total vs. Al_{tot} for samples with discrete chlorite and regular mixed-layer chlorite/smectite. Ornamentation as for Fig. 10.

have a mixture of discrete chlorite and two types of mixed-layer chlorite/smectite. Forty-two analyses of the mafic phyllosilicates in these samples show a considerable compositional range. For sample 455, a wide spread is seen in the noninterlayer and interlayer cation totals, which range from 19.1 to 19.9 and 0.0 to 0.45, respectively (Figs. 10, 11), and also in the x values, which range from 0.5 to 0.95. Analyses of the radiating green phase that infills vesicle centers (illustrated in Fig. 1) are shown as closed squares in Figure 10. The green phase with slightly higher birefringence occurring dominantly in the matrix is represented by closed circles, and analyses of vesicle rims, which also show slightly high birefringence, are shown as triangles.

Analyses from samples 415 and 444 also show considerable ranges in chemical variation (Figs. 10, 11), although they are not as extensive as for sample 455, if the two most smectite-like analyses are excluded in the case of sample 444. The trends shown by these samples are suggestive of a continuous range in chemical character from a near-ideal chlorite type to one more characteristic of a mixed-layer chlorite/smectite with a high chlorite content.

Random mixed-layer chlorite/smectite. Ten analyses of the orange-brown phyllosilicate in samples 430 and 464, in which this phase is the only phyllosilicate present, show they are distinctive from those of pure chlorite or regular mixed-layer chlorite/smectite in having higher SiO_2 and lower Al_2O_3 contents (Table 1). These differences are also apparent in terms of lower noninterlayer cation and higher interlayer cation totals (Figs. 12, 13), as well as low x values. The samples show x values of <0.20 and noninterlayer cation totals of 18–18.5, although four of the analyses lie above these limits. Interlayer cation contents are >0.4, in contrast to the other phyllosilicate phases described above, in which the values are generally <0.4.

Interpretation of analytical investigations

Chlorite compositions

Where analyses of discrete chlorite cluster (samples 413, 426, 447, and 437, Figs. 7, 8) there is little difficulty in taking a mean value to identify the relevant chlorite composition. In other samples there is considerable chemical diversity, however, and identification of phase compositions is less straightforward.

Chlorite analyses for sample 467 plot in two groups, with the group having the lower cation totals plotting in a trend from the chlorite data involving both decreasing noninterlayer totals and increased Al contents (Fig. 9). Part of this trend can be attributed to a degree of mixing between chlorite and celadonite, support for which is also provided by a notable difference in the K_2O contents of the two chlorite groups. The near-ideal chlorite samples have K_2O contents below detection limit, whereas in the second group K_2O averages 0.34%, which largely accounts for the high interlayer contents (Fig. 8). Such high K_2O contents are not present in other chlorite analyses in this study, although K_2O is, of course, a principal component in celadonite. Recalculation of the mean of the second group of analyses so that all the K_2O is removed as a celadonite component gives noninterlayer and interlayer cation totals of 19.6 and 0.3, respectively, compared with the original values of 19.1 and 0.4. These values are in the same range as analyses from other samples, in which only discrete chlorite is thought to be present.

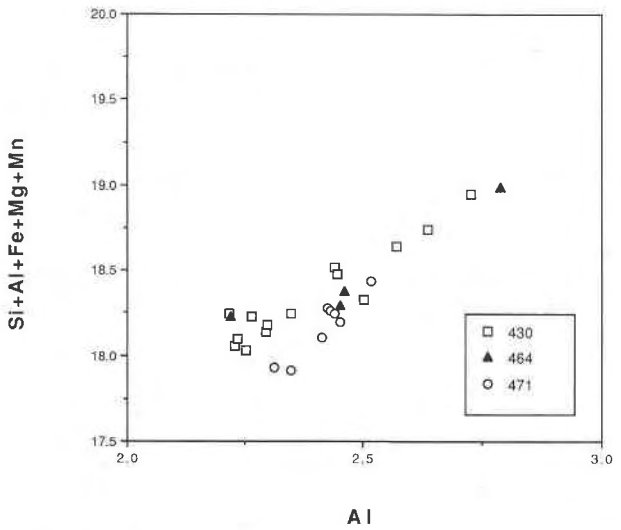

Fig. 12. Noninterlayer cation total vs. Al_{tot} for samples having random mixed-layer chlorite/smectite (samples 430, 464, and 471).

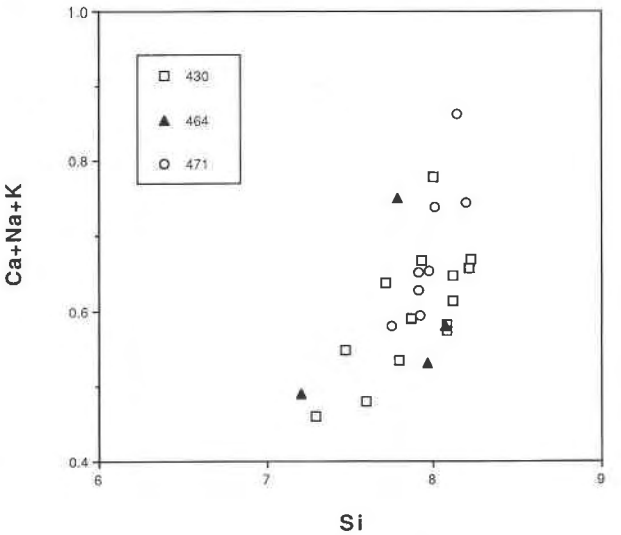

Fig. 13. Interlayer cation total vs. Al_{tot} for samples having random mixed-layer chlorite/smectite (samples 430, 464, and 471).

The XRD pattern for sample 467 indicates that the chlorite and celadonite show only a minimum of mixed layering. The two populations in the chlorite analyses for sample 467 are therefore interpreted as representing, first, a grouping of near-ideal chlorite and, second, a grouping of nonideal chlorite compositions that represent fine intergrowth of chlorite and celadonite. The intergrowth of these two phases must be at a grain size that is beyond resolution by the microprobe, and as a consequence mixed analyses are obtained from such material. A representative chlorite composition can, therefore, only be gained from a mean of the first group of analyses.

A comparable feature is seen in sample 471, in which there is an almost continuous trend in analyses from near-ideal chlorite toward saponite (Fig. 9). If total reliance were placed on the microprobe analyses, such a trend would suggest a near-continuous range from saponite through mixed-layer chlorite/smectite to chlorite. However, as indicated earlier, XRD and petrographic results suggest the presence only of near-ideal chlorite and a random mixed-layer chlorite/smectite with ca. 25% of the chlorite component; thus a continuous trend is not regarded as realistic. If the one analysis central between the two groups in this sequence is omitted, then the mean of each of the two groups can be taken as representative of the compositions of the two types. However, there still remains a considerable spread within the chemical characters of these groups, and the reason for that is not known. It may represent analytical variation or physical intergrowth causing difficulty in obtaining a true analysis of the individual phases present. A further explanation may be that the data are representative of interlayering between packets of chlorite and corrensite, as in the model of Shau et al. (1990). Such interlayering is beyond the resolution of both the microprobe and XRD.

Chlorite and regular mixed-layer chlorite/smectite compositions

Samples with coexisting chlorite and regular mixed-layer chlorite/smectite, as identified by XRD, have microprobe analyses that are closely grouped and appear to suggest a continuous variation between chlorite and mixed-layer varieties. In the case of sample 455, the range in noninterlayer cations from 19.1 to 19.9 is suggestive of a range from a chlorite content of ca. 60 to near 100%. If these analyses were indeed representative of a sequence in which the smectite content varies continuously, then it would not be possible to resolve specific peaks in the XRD patterns representative of a particular chlorite/smectite ratio and that of a near-ideal chlorite. On the basis of the identification by XRD of two varieties of chlorite/smectite and of chlorite, however, the groupings in the analyses of sample 455 can be used to estimate their compositions. For sample 455, a group of seven analyses shows high noninterlayer and low interlayer cation totals (>19.7 and <0.12, respectively; solid squares, Figs. 10, 11) and high x values (>0.84). In contrast, a second group of five analyses shows lower noninterlayer, higher interlayer cation totals (<19.2 and typically >0.3, respectively; solid circles, Figs. 10, 11) and lower x values (<0.6). The remaining nine analyses form a grouping that is intermediate between these two end-members (triangles, Figs. 10, 11).

These groupings accord well with the XRD data, in which two types of chlorite/smectite (with chlorite contents of 65 and 85%) and chlorite are present. If these groupings are taken as representative of the three phyllosilicate types, the ideal noninterlayer cation totals for chlorite/smectite and chlorite should be 19.24 (Chl 65%), 19.67 (Chl 85%), and 20 for chlorite, which compares

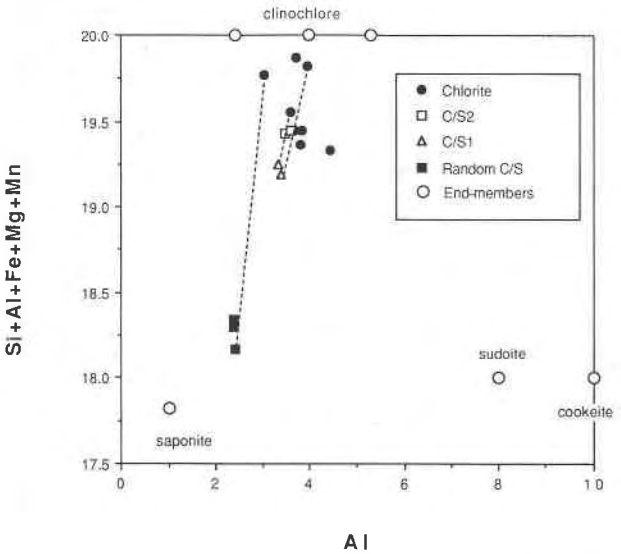

Fig. 14. Mean noninterlayer cations vs. Al_{tot} content for identified discrete chlorites, two types of regular mixed-layer chlorite/smectite, and a random mixed-layer chlorite/smectite. Labeled large circles are end-member compositions taken from Bailey (1988). Dashed lines join phases that occur in the same sample.

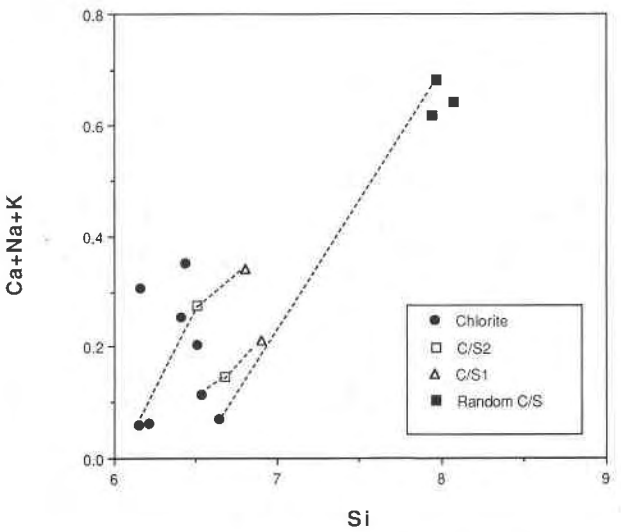

Fig. 15. Mean interlayer cations vs. Si content for identified discrete chlorites, two types of regular mixed-layer chlorite/smectite, and a random mixed-layer chlorite/smectite. Dashed lines join phases that occur in the same sample.

with the observed averages of the three groupings at 19.13, 19.38, and 19.75, respectively. If the mixed layering were in the form of the Shau et al. (1990) model involving a chlorite/corrensite structure, then the equivalent noninterlayer cation totals would be higher, at 19.41, 19.8, and 20.0. The closer match to the chlorite/smectite compositional model offers additional support to that of the XRD data of a chlorite/smectite rather than a corrensite structure.

The XRD pattern for sample 415 was interpreted by Robinson and Bevins (in preparation) to consist of an assemblage similar to that of sample 455, with discrete chlorite and two types of mixed-layer chlorite/smectite, with 60 and 80% chlorite. The analyses from this sample also form three groups (Fig. 10), although the distinction is not as clear as in sample 455. A group of six analyses appears to represent the chlorite/smectite (60:40) type, as they are very similar to the chlorite/smectite (65:35) points in sample 455. However, the remaining seven analyses plot across the area on Figure 10 occupied by the points taken as representative of the chlorite/smectite (85:15) from sample 455, but they do not reach the high noninterlayer cation totals recorded by sample 455 (Fig. 10). Sample 444 shows a scatter of analyses and does not show the higher or lower values; accordingly, recognition of discrete compositions is not possible.

Random mixed-layer compositions

Analyses of the random mixed-layer chlorite/smectite show relatively close groupings in the three samples containing this phase, such that the mean of each of the groupings is taken as a representative composition.

General compositional relationships

Figures 14 and 15 show the mean compositions of eight chlorite, four types of mixed-layer chlorite/smectite, and three random mixed-layer chlorite/smectite samples identified as detailed above. Five of the eight mean analyses of chlorite have fewer noninterlayer cations (<19.75) than an ideal trioctahedral chlorite (Fig. 14), high interlayer cations (0.12–0.42, Fig. 15) and consequently low x values. The XRD results for all these eight samples suggest that there is a minimum (<10%) of mixed-layer smectite content in the chlorite. In contrast, however, on microprobe-determined chlorite values only sample 467 has an x value that is compatible with the XRD data ($x = 0.92$, $1\sigma = 0.05$); rather the majority of chlorite analyses have much lower x values ranging between 0.66 and 0.76. Similar discrepancies between microprobe-determined and XRD-measured chlorite contents have been reported by Bettison and Schiffman (1988) and Schiffman and Fridleifsson (1991), the latter indicating that microprobe-determined chlorite contents of up to 50% were not identified by XRD. In trying to identify the reasons for this discrepancy there are two features to be examined.

First, the mean chlorite analyses do not show a trend toward the saponite point, involving lower noninterlayer cation totals and lower Al totals (Fig. 14), as would be expected if they contained a variable swelling mixed-layer component, as is suggested by their microprobe-determined x values. Such a trend, for example, is well displayed by analyses from sample 471, shown in Figure 9. Rather, there is more of a scatter with respect to Al, with a trend towards di-, tri-chlorites in which there is some dioctahedral character to the chlorite compositions. Such compositions are represented by the ideal cookeite and

sudoite points shown in Figure 14 (Bailey, 1988), involving lower cation totals, but higher Al contents. Such a trend is supported by a correlation between increasing nontetrahedral Al and decreasing x values. In these cases, the calculation of x values gives results that are too low because of the assumption of a trioctahedral (saponitic) composition of the phyllosilicate.

Second, the interlayer cation contents for the eight chlorite samples, in which XRD-determined smectite content is <10%, varies between 0.42 and 0.06 (Fig. 15), whereas for true chlorite it is normal for this value to be near zero. The relatively high contents (>0.2) for four mean analyses of this group (Fig. 15) will also result in lowered x values and noninterlayer cation totals. Schiffman and Fridleifsson (1991) suggested that the recognition of chlorite is unequivocal from microprobe analyses. Such minerals have Si contents of <6.25 per 28 O atoms (Bettison and Schiffman, 1988) and a minimal content of interlayer cations, with increasing Si content being strongly correlated with increasing interlayer cations (Schiffman and Fridleifsson, 1991). Such a correlation is seen in the analyses for samples containing the regular and random mixed-layer chlorite/smectite, as shown in Figures 8 and 13, but no such trend is seen for the discrete chlorite plotted in Figures 8 and 15. These analyses show no correlation between Si and interlayer cations; instead there is a variable range in interlayer cation totals for Si contents of between 6 and 7 pfu. The reason for the very variable interlayer cation totals in chlorite with <10% mixed layers (XRD determined) cannot be determined, however, with the data presently available.

However, from the evidence presented earlier, it is believed that unresolved physical intergrowth of chlorite with other phases such as calcite, mixed-layer chlorite/smectite, and celadonite plays a role. Microprobe determination alone of mixed-layer content must thus be treated with some degree of caution. Similar problems with variable Ca + Na + K contents in chlorite have been reported by others, and Foster (1962) in a review of chlorite disregarded any analyses where these totals were >0.5 wt%. Ernst (1983), in his analysis of chlorite from low-grade metabasalts from Taiwan, noted variable contents of these elements and attributed this also to submicroscopic intergrowth, in this case with phengite, margarite, and paragonite. In the chlorite examined here, neither mixed layering nor physical mixing of the chlorite with other components is entirely satisfactory as an explanation of the anomalous compositions.

In either case the proportions of interlayering or physical contamination necessary to give the interlayer cation totals observed would be at levels (up to 30%) that would be readily determined by XRD, as was demonstrated earlier in the case of sample 455. In addition, such physical or mixed layering would result in a coupled trend between interlayer cations and Si contents, which is clearly not applicable for the discrete chlorite in these samples (Figs. 8, 15). The simplest explanation for the anomalous discrete chlorite compositions is that calcite was a contaminant in these analyses. For example, contamination of the mean chlorite analysis for sample 467 by only 5% calcite would be sufficient to lower the determined noninterlayer cation total and x values from 19.93 and 0.92 to 19.34 and 0.67, respectively. These latter values are in the typical range for discrete chlorite from samples 413, 426, 447, and 437.

Thus, the departure of these points from an ideal trichlorite position with lower noninterlayer cation totals is interpreted as a result of some dioctahedral character and unresolved physical intergrowth of calcite, which is compatible with the XRD data for these samples that are indicative of a near-pure chlorite with a minimum of mixed layering.

Mafic phyllosilicates in metabasite parageneses

Several examples of a progressive sequence of temperature zones that are dominated by certain types of mafic phyllosilicate minerals have been reported from active geothermal systems. The main examples are from Iceland, where smectite-dominated assemblages are typically found below 180–200 °C (Kristmansdóttir, 1979; Schiffman and Fridleifsson, 1991) and discrete chlorite is dominant from about 240 °C (Kristmansdóttir, 1979), although Schiffman and Fridleifsson (1991) reported a slightly higher temperature of 270 °C. At intermediate temperatures mixed-layer chlorite/smectite is dominant, with random structures appearing at lower temperatures (<240 °C, Schiffman and Fridleifsson, 1991) and regular mixed-layers at the higher temperatures. In the regionally metamorphosed Zig-Zag Dal sequence a similar progressive sequence is recognized. Where two or more mafic phyllosilicates coexist, the more smectitic variety always occurs early, as is shown, for example, in Figure 1, where the regular chlorite/smectite is found as a matrix and vesicle rim phase and the chlorite as a later vesicle infilling. A similar feature is recorded for sample 471, in which the random chlorite/smectite occurs in a vesicle rim position, and the chlorite as a later vesicle core infill.

The progressive sequence in mafic phyllosilicates recorded here is from random mixed-layer chlorite/smectite with 25% chlorite to four types of chlorite/smectite with chlorite contents of 60, 65, 80, and 85%. The recognition of four types of chlorite/smectite with very similar contents of chlorite suggests that the transition from smectitic to chloritic phyllosilicates proceeds in a gradual transition and not in discrete steps. This is in agreement with the conclusions of Bettison and Schiffman (1988) and Bettison-Varga et al. (1991), who argued on the basis of microprobe-determined compositions for a continuous range of chlorite contents of between 50 and 100%.

The mafic phyllosilicate assemblages found in the Zig-Zag Dal basalt section are random chlorite/smectite + discrete chlorite and two types of chlorite/smectite (high chlorite contents) + discrete chlorite. Such variety occurs in an irregular fashion within a 1300-m vertical section, which is suggestive of nonequilibrium conditions prevailing in those rocks. That was also a conclusion of Bettison-Varga et al. (1991), who found a similar variety in

mafic phyllosilicate assemblages from the Point Sal Ophiolite in California.

As chlorite is a ubiquitous mineral at very low-grade and low-grade metamorphism, it is taken as an in-excess phase in model systems, and projection is made from chlorite with a fixed composition, typically of an ideal clinochlore type (Liou et al., 1985; Frey et al., 1991). Frey et al. (1991) further investigated the effects of solid solution in low-grade minerals, including chlorite, pumpellyite, prehnite, and actinolite, on the simplified petrogenetic grid of Liou et al. (1985). They calculated the clinochlore activities for 118 chlorite analyses from 19 data sources, which gave an average of 0.053 ($1\sigma = 0.044$). Activity values for the mean compositions from this study have been calculated using the same ideal site mixing model (Holland and Powell, 1990), which show a range from 0.005 to 0.070, with a mean of 0.029 ($1\sigma = 0.022$). Almost the same range is observed here in chlorite activities as for the 1σ deviation presented by Frey et al. (1991) for chlorite from many different areas. No details of activity ranges were given for individual areas by Frey et al. (1991), and so it is not possible to assess whether the range in clinochlore activities seen here is typical. Using their average clinochlore activity value, Frey et al. (1991) demonstrated that the various low-grade mineral stability fields are highly variable and that extensive overlap of the subgreenschist facies fields occurs. The wide range in the clinochlore activities identified in the chlorite samples from the Zig-Zag Dal basalt sequence is one of the reasons for the cause of the variability in mineral assemblages observed, and indeed this feature of extensive facies overlap is no doubt more prevalent than generally acknowledged.

Conclusions

Mafic phyllosilicates in very low-grade metabasites from the Zig-Zag Dal Basalt Formation have been shown on optical, microprobe, and XRD evidence to be highly varied in their chemical and structural properties. Phases include chlorite, two types of regular mixed-layer chlorite/smectite, random mixed-layer chlorite/smectite, and celadonite. Major chemical variation in some samples is attributed to fine-grained physical intergrowths between various minerals such that the optical and microprobe results are suggestive of a gradual continuum between phases rather than discrete phases.

In those minerals recognized by XRD as having a mixed-layer chlorite/smectite character, there is a close correspondence between the XRD-determined smectite content and that determined by recalculation of microprobe analyses. However, several examples occur in which discrete chlorite recognized by XRD is shown as having variable content of swelling component as calculated from microprobe data. Much of this discrepancy can be attributed to the resulting erroneous analyses obtained from material in which unresolved fine-grained physical mixing between other phyllosilicates and calcite is present. Also, the assumption of a trioctahedral character in the microprobe recalculation scheme will result in erroneous estimates of mixed-layer content if any dioctahedral character is evident in the minerals.

Discrete chlorite recognized in the Zig-Zag Dal basalts has a wide range of chemical composition, suggesting that the use of chlorite of a fixed composition (usually clinochlore) as a projection point in model systems for low-grade metabasites may lead to inconsistent analysis of parageneses. The discrete chlorite recognized in these rocks has very low clinochlore activities and a wide range (mean = <0.03, $1\sigma = 0.022$), which will result in considerable variation in the stability fields of accompanying calc-silicate minerals among samples and lead to considerable overlap in P-T space of the mineral facies, based on such calc-silicate assemblages as those modeled recently by Frey et al. (1991).

Acknowledgments

This paper is published with the permission of the Geological Survey of Greenland. H.F. Jepsen is thanked for making the samples available. P. Schiffman, D.R. Peacor, and Y.-H. Shau are thanked for their constructive criticisms on a first draft of the manuscript, which prompted a reappraisal of some aspects of the interpretation.

This paper is a contribution to IGCP Project 294, Very Low Grade Metamorphism.

References cited

Bailey, S.W. (1982) Nomenclature for regular interstratifications. American Mineralogist, 67, 394–398.

——— (1988) Chlorites: Structure and crystal chemistry. In Mineralogical Society of America Reviews in Mineralogy, 19, 347–403.

Bettison, L.A., and Schiffman, P. (1988) Compositional and structural variations of phyllosilicates from the Point Sal Ophiolite, California. American Mineralogist, 73, 62–76.

Bettison-Varga, L.A., Mackinnon, D.R., and Schiffman, P. (1991) Integrated TEM, XRD and electron microprobe investigation of mixed-layered chlorite/smectite from the Point Sal Ophiolite, California. Journal of Metamorphic Geology, 9, 697–710.

Bevins, R.E., Robinson, D., and Rowbotham, G. (1992) Zeolite facies metamorphism of the late Proterozoic Zig-Zag Dal Basalt Formation, eastern North Greenland. Lithos, 27, 155–165.

Buckley, H.A., Bevan, J.C., Brown, K.M., and Johnson, L.R. (1978) Glauconite and celadonite: Two separate mineral species. Mineralogical Magazine, 42, 373–382.

Cho, M., and Liou, J.G. (1987) Prehnite-pumpellyite to greenschist facies transition in the Karmutsen metabasites, Vancouver Island, B.C. Journal of Petrology, 27, 467–494.

Cho, M., Maruyama, S., and Liou, J.G. (1986) Transition from the zeolite to prehnite-pumpellyite facies in the Karmutsen metabasites, Vancouver Island, B.C. Journal of Petrology, 27, 467–494.

Ernst, W.G. (1983) Mineral parageneses in metamorphic rocks exposed along Tailuko Gorge, Central Mountain Range, Taiwan. Journal of Metamorphic Geology, 1, 305–329.

Foster, M.D. (1962) Interpretation of the composition and a classification of the chlorites. U.S. Geological Survey Professional Paper, 414A, 22 p.

Frey, M., de Capitani, C., and Liou, J.G. (1991) A new petrogenetic grid for low grade metabasites. Journal of Metamorphic Geology, 9, 497–509.

Holland, T.J.B., and Powell, R. (1990) An enlarged and updated internally consistent thermodynamic dataset with uncertainties and correlations: The system K_2O-Na_2O-CaO-MgO-MnO-FeO-Fe_2O_3-Al_2O_3-TiO_2-SiO_2-C-H_2-O_2. Journal of Metamorphic Geology, 8, 89–124.

Hower, J. (1981) X-ray identification of mixed-layer clay minerals. In Mineralogical Association of Canada Short Course Handbook, 7, 39–59.

Jepsen, H.F., Kalsbeek, F., and Suthren, R.J. (1980) The Zig-Zag Dal

Basalt Formation, North Greenland. Rapport Grønlands geologiske Undersogelse, 99, 25–32.

Kalsbeek, F., and Jepsen, H.F. (1984) The late Proterozoic Zig-Zag Dal Basalt Formation of eastern North Greenland. Journal of Petrology, 25, 644–664.

Kristmansdóttir, H. (1975) Clay minerals formed by hydrothermal alteration of basaltic rocks in Icelandic geothermal fields. Geologiska Föreningens i Stockholm Förhandlingar, 97, 289–292.

——— (1979) Alteration of basaltic rocks by hydrothermal activity at 100–300°C. In M. Mortland and V. Farmer, Eds., Developments in sedimentology, 27, p. 359–367. Elsevier, Amsterdam.

Liou, J.G., Maruyama, S., and Cho, M. (1985) Phase equilibria and mineral parageneses of metabasites in low grade metamorphism. Mineralogical Magazine, 49, 321–333.

Reynolds, R.C. (1985) NEWMOD©: A computer program for the calculation of one-dimensional diffraction patterns of mixed layered clay minerals. R.C. Reynolds, 8 Brook Rd, Hanover, New Hampshire 03755, U.S.A.

——— (1988) Mixed layer chlorite minerals. In Mineralogical Society of America Reviews in Mineralogy, 19, 601–629.

Schiffman, P., and Fridleifsson, G.O. (1991) The smectite to chlorite transition in drillhole NJ-15, Nesjavellir Geothermal Field, Iceland: XRD, BSE and electron microprobe investigations. Journal of Metamorphic Geology, 9, 679–696.

Shau, Y.-H., and Peacor, D.R. (1992) Phyllosilicates in hydrothermally altered basalts from DSDP Hole 504B, Leg 83: A TEM and AEM study. Contributions to Mineralogy and Petrology, 112, 119–133.

Shau, Y.-H., Peacor, D.R., and Essene, E.J. (1990) Corrensite and mixed-layer chlorite/corrensite in metabasalt from northern Taiwan: TEM/AEM, EMPA, XRD and optical studies. Contributions to Mineralogy and Petrology, 105, 123–142.

Manuscript received August 27, 1991
Manuscript accepted November 15, 1992